Journal of Bone Oncology 29 (2021) 100366

Contents lists available at ScienceDirect

Journal of Bone Oncology

journal homepage: www.elsevier.com/locate/jbo

Research Paper

Preoperative CT for prediction of local recurrence after curettage of giant cell tumor of bone

Lenian Zhou [a,1], Shanyi Lin [a,1], Hanqiang Jin [a], Zhaoyuan Zhang [a], Changqing Zhang [a,b,*], Ting Yuan [a,*]

[a] Department of Orthopaedics, Shanghai Jiao Tong University Affiliated Sixth People's Hospital, 600 Yishan Road, Shanghai 200233, China
[b] Institute of Microsurgery on Extremities, Shanghai Jiaotong University Affiliated Sixth, People's Hospital, Shanghai, 200233, China

1. Introduction

Giant cell tumor of bone (GCTB) is an intermediate, locally aggressive tumor that generally localizes to the *meta*-epiphyseal regions of long bones [1]. GCTBs comprise approximately 5% of all bone tumors and occur primarily in younger persons aged 20 to 45 years [2]. While GCTBs rarely metastasize, they have a tendency to recur locally [3]. Various demographic, clinical, and therapeutic factors contribute to the recurrence of GCTBs [4]. Increased recurrence is seen in patients younger than 25 years [5], for locations in the distal radius and proximal femur [6–9], and in cases of secondary aneurysmal bone cysts (ABC) [10].

The most commonly used radiological classification system is the Campanacci system [11], which classifies GCTBs into three types based on tumor appearance on standard x-ray radiographs. Although the Campanacci grading system has been used for decades, many studies have found that it provides limited prognostic information about recurrence of GCTBs [5,6]. Since the Campanacci system is based solely on interpretation of complex morphologies in two-dimensional (2-D) radiographs, it is difficult to identify tumor borders precisely [12], leading to a potential observer bias. As a result, large tumor-grading variance has been reported among raters using the Campanacci classification, especially for grade II and grade III tumors [13].

Computed tomography (CT) is valuable in evaluation of musculoskeletal tumors, because it can clearly show bone resorption and destruction of cortical and subchondral bone within the lesion [14]. With preoperative CT, surgeons can see more anatomical details for establishing a surgical plan, improving precision of tumor removal and accuracy of reconstruction in tumor surgeries [15]. However, the prognostic value of preoperative CT images for GCTBs has not been adequately evaluated. In addition to limited sample sizes, most previous studies have had many methodological problems. Simply based on a qualitative approach instead of a specific criterion, patients with cortical-bone involvement on CT images showed a higher recurrence rate than patients with non-involvement in terms of absolute difference (>30%), although this difference did not reach statistical significance [16]. By using a relatively arbitrary definition on subchondral bone involvement, Chen et al. [17] found no significant association between subchondral bone involvement (distance from the tumor edge to the articular surface < 3 mm) and prognosis. Likewise, Prosser et al. [13] observed a large absolute but statistically insignificant difference in recurrence rate among groups with different tumor-articular distances (<1 mm, 17.4% vs. > 5 mm, 0%). To overcome these shortcomings, we studied a large sample of patients and used a refined approach to analyze preoperative CT images of GCTBs and ROC analysis to predict recurrence. We found reasonable cut-off points for recurrence for these previously reported features of GCTBs.

We asked the following research questions: (1) Do preoperative CT images of GCTBs have value in prognostic prediction? (2) Which features of GCTBs on CT images, are related to recurrence?

2. Methods

2.1. Data source and patient selection

We retrospectively reviewed the records of all patients who underwent extended curettage for GCTB with relevant CT imaging records (n = 300) in our hospital (Shanghai Sixth People's Hospital affiliated with Shanghai Jiao Tong University, Shanghai, China) from November 2010 through October 2018. All patients received a histopathologic diagnosis of GCTB. Follow-up time was at least 24 months. We excluded patients diagnosed with malignant GCTB (n = 6) and patients lost to follow-up (n = 83). A total of 211 patients (101 women; 110 men) were included for analysis. The average follow-up time was 62.5 months (range: 24–119 months), and the average patient age at surgery was 34.7 years (range: 14–72 years). There were 173 cases of primary GCTB (82.0%), 38 cases of recurrent GCTB (18.0%), and 31 cases of pathological fracture (14.7%). GCTBs were graded according to the Campanacci et al. classification [11].

All patients included underwent extended curettage in a similar surgical procedure performed by four surgical teams. Briefly, a large window over the affected bone was opened to access the tumor. A set of curettes was used to remove the visualized lesion. For recurrent cases, the remaining bone graft/cement, if existed,

* Corresponding authors at: Department of Orthopaedics, Shanghai Jiao Tong University Affiliated Sixth People's Hospital, 600 Yishan Road, Shanghai 200233, China (T. Yuan). Institute of Microsurgery on Extremities, Shanghai Jiaotong University Affiliated Sixth, People's Hospital, Shanghai, 200233, China (C. Zhang).
E-mail addresses: zhangcq@sjtu.edu.cn (C. Zhang), terrenceyuan@gmail.com (T. Yuan).
[1] Lenian Zhou and Shanyi Lin contributed equally to this article.

https://doi.org/10.1016/j.jbo.2021.100366

was also removed for potential tumor involvement. Then, the residual bone cavity was extended with high-speed burring and was flushed with sterile saline for better visualization. Next, the exposed bone cavity was treated with an adjuvant, either phenol or alcohol, to minimize local recurrence. Finally, the cavity was filled with autologous bone (e.g., autologous iliac bone), allogeneic bone, or bone cement. The surgeon and patient discussed treatment options and then decided on the method of cavity reconstruction. For cases reconstructed with "cement + bone graft", bone graft was first implanted at the subchondral region followed by cementation of the cavity. Of the included patients, 165 received a bone graft (autologous or allogeneic), 26 received a bone graft and bone cement, and 20 received bone cement only.

Patient information and data were collected from the hospital's clinical inpatient database system and medical records. The Ki-67 proliferative index, used to evaluate the growth fraction of neoplastic cell populations [18], was assessed on the diagnostic biopsy, or when biopsy was not performed, on the surgical specimen. Patients received follow-up through clinic visits, via telephone call, or via WeChat (instant messaging software). Clinic visits were recommended 1, 3, 6, and 12 months after surgery, and annually thereafter. X-ray evaluations were obtained in postoperative examinations and additional enhanced MRI was performed when local recurrence was suspected.

With GCTBs, adjuvant therapy (e.g., denosumab, bisphosphonates) is commonly used to reduce the risk of tumor recurrence or metastasis [19,20]. In the present study, 42 patients were treated preoperatively with denosumab, and 32 patients were treated postoperatively with denosumab. Twenty-one patients received postoperative bisphosphonate therapy. The details of denosumab and bisphosphonate treatment are not available in our follow-up.

2.2. Measurement of tumor parameters

Preoperative CT examinations were performed with using one of three CT scanners (Discovery CT 750 HD, GE Healthcare, CHICAGO, IL, USA; Brilliance 64, Philips, Amsterdam, Netherlands; and SOMATOM Force, Siemens AG, Erlangen, Germany), and high-resolution CT images obtained using a slice thickness of 0.625 mm. In CT images, we measured (1) tumor size, (2) distance between the tumor edge and articular surface, (3) thickness of thinnest part of the cortex affected by the tumor, and (4) thickness of unaffected bone cortex. First, we visually inspected CT images of the tumor in coronal, sagittal, and transverse planes, searching for the coronal and sagittal CT sections that showed the tumor's edge closest to the articular surface. In those two sections, we then measured the shortest distance between the edge of the tumor to the subchondral bone of the articular surface. The smaller of the two values was recorded as the tumor-articular surface distance (Fig. 1). For recurrent cases, remaining bone graft was also considered as a part of tumor when we determined the edge between tumor and surrounding normal bone tissue.

The thickness of the thinnest part of the cortex affected by the tumor and the thickness of distal unaffected bone cortex to the articular surface around the tumor were similarly measured in transverse CT sections. First, we visually inspected all transverse CT images of the tumor until we found the section containing the thinnest cortex affected by the tumor. In that section, we measured the thickness of the thinnest cortex and recorded this value (Fig. 2). In cases in which the affected cortical or subchondral bone was not continuous, the thinnest cortical thickness affected by the tumor or the tumor–articular surface distance was recorded with a value of 0 (Fig. 2C and Fig. 1C).

To measure the thickness of distal unaffected bone cortex to the articular surface around the tumor, we first visually inspected coronal CT sections to identify the tumor edge away from the articular surface (Fig. 3A, C), and then identified the cross-sectional CT images (axial view) (Fig. 3B, D); these are indicated virtually by the red-dashed lines in Fig. 3A, C. Finally, we found two tangent points between tumor edge and cortical bone on cross-sectional CT images, and measured the thicknesses of distal cortex to the articular surface *not* affected by the tumor at those two points. The average of the two measurements represents the thickness of unaffected cortical bone around the tumor.

These four parameters were measured independently by two orthopedic oncologists with expertise in evaluating radiographs. For each case, the measurements of the two observers were averaged, and this average value was taken as the final recorded value for the given parameter. The observers were blinded to the patients' clinical information. If the two observers disagreed on the choice of CT section on which to make the measurements, they discussed the case until they arrived at a consensus.

2.3. Statistical analysis

First, we conducted a univariate analysis of all possible risk factors on recurrence (yes/no), and noted which tumor measurement parameters were related to recurrence. We used Student's *t*-test and Pearson's chi-square test to compare differences between continuous and categorical variables, respectively. Receiver operating characteristic (ROC) curves were used to analyze continuous variables (such as age, distance from the tumor edge to the articular surface, and the thickness of unaffected bone cortex around the tumor). We used the Youden index to determine the best cut-off point in the ROC analysis. Multivariable logistic regression analysis with variable selection determined by the Akaike Information Criterion (AIC) [21] was used to identify the final factors that best predicted recurrence; the concordance index (C-index) of the model was also calculated. Generally, the quality range of C-indices can be categorized into 5 levels: excellent (0.9–1.0); good (0.8–0.89); fair (0.7–0.79); poor (0.6–0.69); or no ability to distinguish (0.5–0.59) [22]. We also conducted sensitivity analyses to assess the stability of statistical analyses by respectively excluding recurrent cases, cases receiving denosumab and/or bisphosphonate. Statistical analysis was performed using SPSS software Version 26 (IBM Corp. Released 2019. IBM SPSS Statistics for Windows, Version 26.0. Armonk, NY: IBM Corp). All tests were two-sided, and p values < 0.05 were taken as significant. Data are presented as means ± standard deviations (SD) unless otherwise indicated. The intraclass correlation coefficients (ICCs) were used to assess the interobserver reliabilities.

3. Results

3.1. Baseline characteristics of the patients

Table 1 presents a summary of patient demographic, clinical, and tumor characteristics at baseline. The overall local recurrence rate was 26.5% (56/211) within an average surgery-recurrence interval of 17.4 ± 11.3 months (range, 3–63 months). Of the 211 patients, 7 (3.3%) had lung metastases. The anatomical locations and frequency of GCBTs in those locations are shown in Table 1. Most of the GCBTs (68.2%) were located around the knee joint (79 in the distal femur, 63 in the proximal tibia, and 2 in the proximal fibula). Histopathology analysis revealed that the GCTB in 59 patients were complicated by aneurysmal bone cysts.

3.2. Analysis of risk factors

Univariate analyses of the demographic and clinical data of the subjects (n = 211) showed that only anatomical location of the

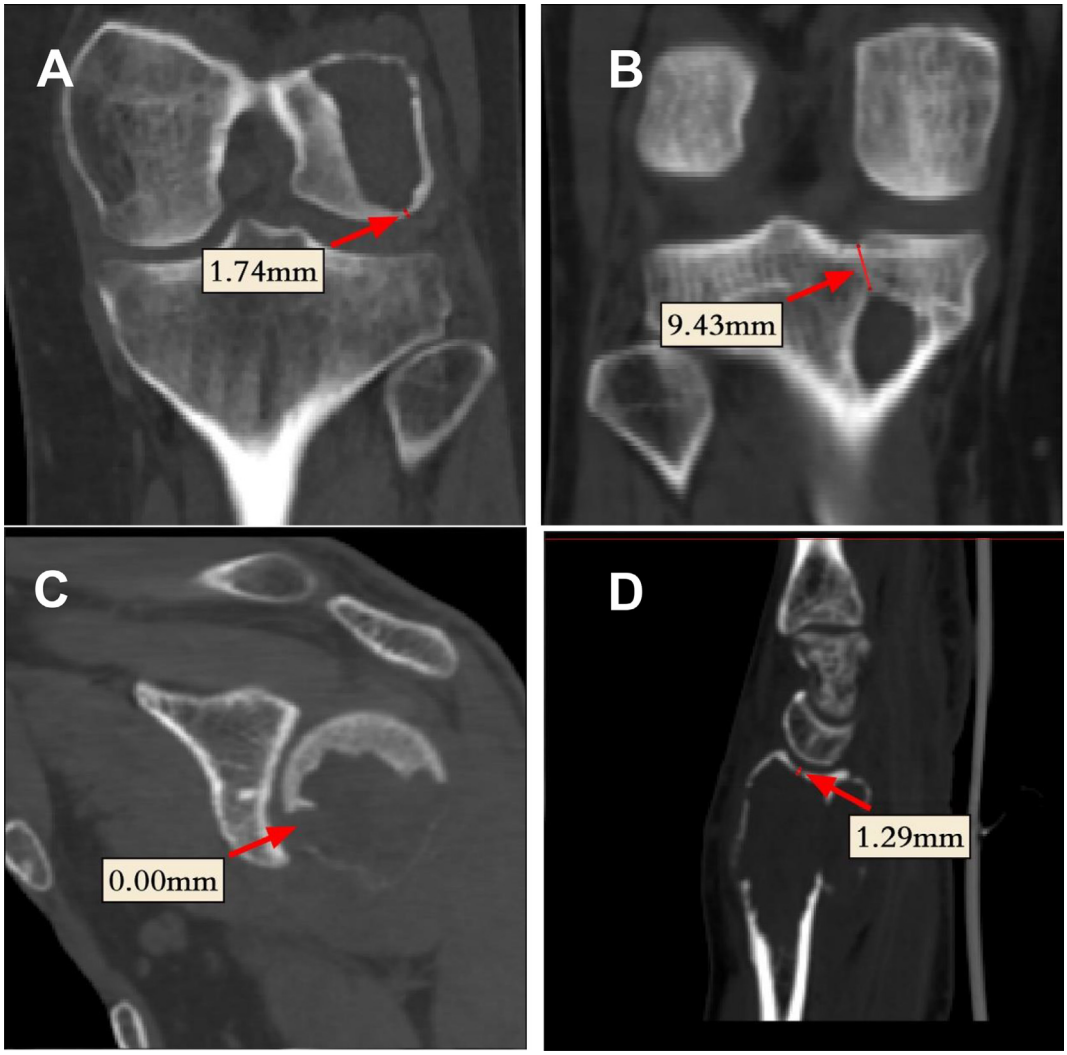

Fig. 1. (A) Coronal CT images of GCTBs in the lateral condyle of the distal femur; (B) proximal tibia; (C) proximal humerus; and (D) sagittal CT image of GCTB in the distal radius. Distance (red line) from the tumor edge to the articular surface is, respectively, AD, 1.74 mm, 9.43 mm, 0 mm, and 1.29 mm. (For interpretation of the references to colour in this figure legend, the reader is referred to the web version of this article.)

tumor (Pearson's chi-square, p = 0.004) was significantly related to recurrence (Table 1). No other patient variables in the univariate analyses were related to recurrence. There was also no significant difference in the average follow-up time between patients experiencing recurrence (recurrence group) and those who did not experience recurrence (non-recurrence group) (60.36 months vs. 63.29 months, p = 0.53). On average, patients in the recurrence group were significantly younger than those in the non-recurrence group (30.21 years vs. 36.32 years, p = 0.001). The average Ki-67 proliferative index of the two groups was not significantly different (recurrence, 14.88%; non-recurrence, 14.55%, p = 0.83), and the average tumor size of the two groups was not significantly different (recurrence, 54.41 mm; non-recurrence, 52.00 mm, p = 0.44). In the non-recurrence group, the average thickness of the unaffected bone cortex around the tumor was greater than that in the recurrence group (3.37 vs. 2.60 mm, p < 0.001), as was the average thickness of the thinnest cortex affected by the tumor (0.87 vs. 0.48 mm, p < 0.001). In the non-recurrence group, the average distance from the tumor edge to the articular surface was also greater (3.29 vs. 1.31 mm, p = 0.025) (Table 1). For these four above-mentioned indicators, ICCs for interobserver reliability were 0.91, 0.87, 0.91, and 0.97, respectively.

To determine which combination of risk factors was associated with GCTB recurrence, we used multivariate logistic regression analysis. According to the best multivariate prognostic model based on AIC, the risk factors associated with GCTB recurrence were distance from the tumor edge to the articular surface, thickness of unaffected cortical bone around the tumor, and patient age at surgery (AIC = 57.99). Based on the Youden's Index and ROC curve analysis, the cut-off points for the distance from the tumor edge to the articular surface and the thickness of the unaffected cortical bone around the tumor were 2 mm and 3 mm, respectively.

We stratified patients by age into 4 groups (<20, 20–29, 30–39, and $\geq$ 40) for clinical application. Multivariate logistic regression analysis of four levels of age, distance from the tumor edge to the articular surface, and thickness of unaffected bone cortex around the tumor were independent risk factors for GCTB recurrence after extended curettage (p < 0.05) (Table 2). The C-index of the final model was 0.82 (CI, 0.76 to 0.88), which suggests that these three factors reliably predict the recurrence of GCTB [22]. In sensitivity analyses (excluding patients receiving denosumab, bisphosphonate and recurrent cases, respectively), there showed no clear difference in trends. (see online appendix).

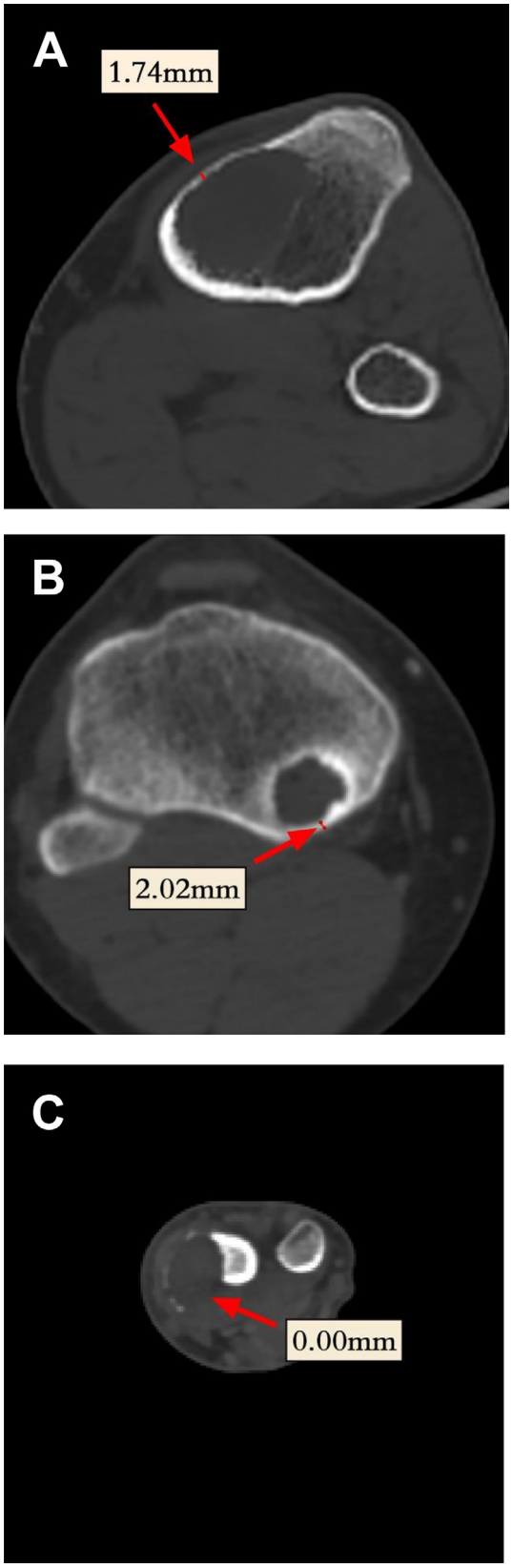

Fig. 2. (A, B) Cross-sectional CT images (axial view) of GCTBs in the proximal tibia, and (c) distal radius. Thickness (red line) of the thinnest cortex affected by the tumor is, respectively, A-C, 1.74 mm, 2.02 mm, and 0 mm. (For interpretation of the references to colour in this figure legend, the reader is referred to the web version of this article.)

4. Discussion

Although moderately aggressive, GCTBs are difficult to treat because of their predilection to arise in the *meta*-epiphyseal regions of long bones and their tendency to recur locally [5]. Since GCTBs occur primarily in young people 20–45 years of age, preserving bone anatomy is paramount. *En bloc* tumor resection is associated with a lower risk of tumor recurrence; however, it has a higher incidence of complications such as mechanical failure, aseptic loosening of the prosthesis, nonunion, and compromised limb function [23–25], which all affect subsequent quality of life. For these reasons and due to advances in surgical techniques and adjuvant therapies, the treatment of choice for GCTBs has increasingly become intralesional curettage instead of *en bloc* resection [26]. Although curettage has a higher recurrence rate than *en bloc* resection [27], maximum limb function is preserved, and integrity of the autogenous joint is retained [28,29].

To perform thorough intralesional curettage and lower the risk of recurrence, it is crucial to accurately identify the tumor's boundaries preoperatively and other tumor-related factors contributing to recurrence, all of which are difficult to do on traditional 2-D radiographs. In the present study, we analyzed features of GCTBs on CT images and in three dimensions, and we used those features along with patient variables to evaluate their predictive power for local tumor recurrence.

CT imaging is commonly used to diagnose and evaluate bone tumors [30]. Tomography can clearly show bone resorption and destruction of cortical and subchondral bone within the lesion, all of which are clearer from that discernable in traditional 2-D radiographs [14,31]. The superiority of CT imaging and its ability to distinguish overlapping structures prompted Campanacci et al. [32] to propose a new CT-based classification method, which they used to assess the risk of GCTB recurrence after denosumab treatment. Using CT and MRI imaging, He et al. [33] also found that tumor cystic changes were an independent risk factor for GCTB recurrence. To the best of our knowledge, our study is the first to employ quantitative measurement of GCTB features on preoperative CT images to evaluate their prognostic value.

Our study found that the distance from the tumor edge to the articular surface is a factor affecting recurrence. Although the precise origin of GCTBs is controversial, GCTBs usually are observed in the metaphysis and extend to the subchondral bone [34,35]. Futamura et al. [36] found that a best-fitting regression model using quantitative CT measurements localized the GCTBs predominantly in the metaphysis. Prosser et al. [13] reported that 96% of lesions are within 5 mm of the articular surface. Chen et al. [17] reported that in most patients the tumor invades subchondral bone when bone thickness is < 3 mm. We found that 95.7% (202/211) of the lesions were<5 mm from the articular surface, and 82.5% (174/211) were<3 mm. With extended curettage, there is only a small amount of bone on the joint side that can be safely scraped away. McGough et al. [37] found that subchondral bone tumors commonly recur. This might be due to a failure to accurately assess the condition of subchondral bone, leading to insufficient removal of lesions around the articular cartilage. Although we assessed the condition of subchondral bone with preoperative CT and removed as much tumor as possible, the proximity of the tumor to the subchondral bone precludes thorough curettage. Suzuki et al. [38] found an inverse correlation between the thickness of subchondral bone and recurrence on the joint side. However, Prosser et al. [13] found that the recurrence rate did not correlate with distance from the articular surface. We reasoned that this apparent discrepancy was due to limited sample size and bias error between measurements done using CT and MRI images.

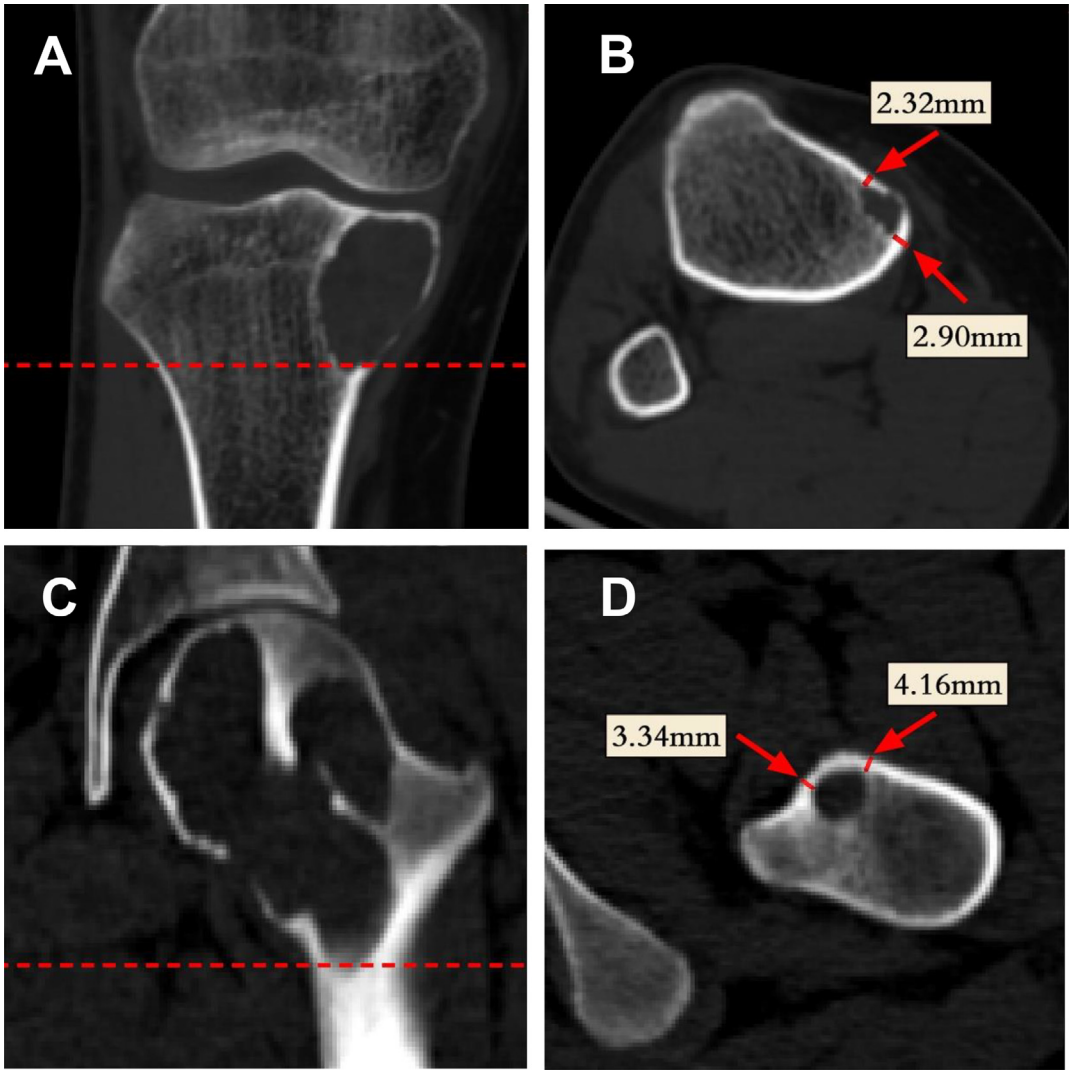

Fig. 3. Quantitative measurements of the thickness (red solid lines) of the unaffected cortical bone around the tumor in CT images of GCTBs in the (A) proximal tibia and (C) proximal femur. The average unaffected cortical thicknesses of the non-invaded part around the tumor is (B) 2.61 mm and (D) 3.75 mm. Panels (B) and (D) are axial images. Dashed red lines in coronal images (A and C) show level at which the axial image in corresponding panels was taken.and (c) distal radius. Thickness (red line) of the thinnest cortex affected by the tumor is, respectively, A-C, 1.74 mm, 2.02 mm, and 0 mm. (For interpretation of the references to colour in this figure legend, the reader is referred to the web version of this article.)

We also determined that the thickness of the unaffected cortical bone around the tumor is an independent risk factor for recurrence, which is consistent with our observation that recurrence is related to anatomical location. The recurrence rate was high (64.7%, 11/17) for GCTBs in the distal radius, a tendency documented previously [7,39,40]. This high rate might be due to the complex anatomy of the distal radius, precluding thorough intralesional curettage. Our study also adds new information related to this finding. We found that at the distal radius cortical thickness is relatively thin around the tumor, which may limit the extent of curettage. Moreover, the median nerve, radial artery, and flexor and extensor tendons need to be avoided when polishing the cortical bone or applying adjuvants. Scraping alone with a curette can thus leave residual tumor on the cortex. Similarly, for tumors in the proximal fibula or distal ulna, the unaffected cortical bone around the tumor is also thinner than other parts, possibly leading to a higher recurrence rate for the same reasons. Since our study sample had too few of these latter cases, this hypothesis needs to be evaluated further. Unlike with the distal radius, in these cases after the tumor is completely removed, functional impairment is minimal [6,24]. The region with the thinnest cortical bone can reflect the degree of tumor invasion, which is also the foundation for Campanacci classification. With this in mind, surgeons could choose a bone window over thinned or perforated bone cortex through which to perform surgery. In this way, no residual tumor would be left on the bone.

Our study had some limitations. First, although we included all consecutive patients to reduce selection bias, as this was a single-center retrospective study, our prediction model lacked external corroboration from other centers or from other populations of patients with GCTBs. Second, patients without preoperative CT imaging records in our hospital were not included in this study. We did, however, accept a large number of referral patients from all over the country, and some of them brought preoperative CT image films. As these films were taken at other hospitals, we were not able to access the digital versions. Under these circumstances, we were still able to include an ample number of these patients, even though referral bias might exist. Third, the patients were evaluated by different models of CT scanners. The CT machines that we used, however, were calibrated daily according to international

Table 1
Univariate analysis of patient (n = 211) demographics and baseline characteristics.

Variable	Recurrence*		P value
	Yes	No	
Sex, No. (%)			
Male	31 (55.4)	79 (51.0)	0.57
Female	25 (44.6)	76 (49.0)	
Tumor location, No. (%)			
Distal femur	19 (33.9)	60 (38.7)	0.004
Proximal tibia	11 (19.6)	52 (33.5)	
Proximal femur	8 (14.3)	15 (9.7)	
Distal radius	11 (19.6)	6 (3.9)	
Proximal humerus	4 (7.1)	5 (3.2)	
Pelvis	1 (1.8)	4 (2.6)	
Other	2 (3.6)	13 (8.4)	
Campanacci classification, No. (%)			
Grade I	1 (1.8)	3 (1.9)	0.12
Grade II	23 (41.1)	88 (56.8)	
Grade III	32 (57.1)	64 (41.3)	
Primary or recurrent, No. (%)			
Primary	46 (82.1)	127 (81.9)	0.97
Recurrent	10 (17.9)	28 (18.1)	
Pathological fracture, No. (%)			
Yes	11 (19.6)	20 (12.9)	0.22
No	45 (80.4)	135 (87.1)	
Secondary ABC, No. (%)			
Yes	17 (30.4)	42 (27.1)	0.64
No	39 (69.6)	113 (72.9)	
Preoperative denosumab, No. (%)			
Yes	16 (28.6)	26 (16.8)	0.058
No	40 (71.4)	129 (83.2)	
Postoperative denosumab, No. (%)			
Yes	6 (10.7)	26 (16.8)	0.28
No	50 (89.3)	129 (83.2)	
Postoperative bisphosphonate, No. (%)			
Yes	4 (7.1)	17 (11.0)	0.41
No	52 (92.9)	138 (89.0)	
Cavity reconstruction, No. (%)			
Cement alone	4 (7.1)	16 (10.3)	0.69
Bone graft alone	46 (82.1)	119 (76.8)	
Cement + bone graft	6 (10.7)	20 (12.9)	
Age, yr (mean ± SD) †	30.21 ± 10.08	36.32 ± 13.61	0.001
Follow-up, months (mean ± SD)	60.36 ± 30.42	63.29 ± 29.53	0.53
Ki-67 proliferative index, % (mean ± SD)	14.88 ± 10.77	14.55 ± 8.20	0.83
Size of tumor, mm (mean ± SD)	54.41 ± 20.72	52.00 ± 19.68	0.44
Distance from the tumor edge to the articular surface, mm (mean ± SD)	1.31 ± 0.91	3.29 ± 6.51	0.025
Thickness of the thinnest cortical layer, mm (mean ± SD)	0.48 ± 0.64	0.87 ± 0.82	<0.001
Thickness of unaffected cortical bone around tumor, mm (mean ± SD)	2.60 ± 0.76	3.37 ± 0.89	<0.001

* Within a minimum follow-up of 24 months, with a mean follow-up of 62.5 ± 29.7 month (24–119 months)
† Age at surgery.

protocols. In order to further evaluate systematic error caused by measurement bias, we consulted engineers of the three CT machines for measuring accuracy, and the measurement error of drawing lines was less than 5% of (measurement distance + 2 mm) on the same machine, which was acceptable in this study. Given all CT images were archived in the hospital's picture archive and communication system (PACS), we believed that the potential variability introduced by this approach was unavoidable and reflects the actual clinical practice in a large hospital over a 9-year study period. Fourth, we only examined whether or not patients underwent denosumab or bisphosphonate treatment. Since denosumab as an adjuvant therapy has only been in use for the last 4 years in China, we did not report the details (dosages and frequencies) of denosumab administration. Because denosumab was not approved for treatment of GCTB in Mainland China during the study period, we relied on patient self-reports to determine if they obtained denosumab in neighboring regions, such as Hong Kong and Taiwan; this might have contributed to recall bias.

Table 2
Results of multivariate logistic regression of factors predicting recurrence after extended curettage.

Variable	Odds Ratio (95% Confidence Interval)	P value
Age		
Under 20	1.59 (0.433–5.836)	0.48
20–29	3.17 (1.255–7.993)	0.015
30–39	1.28 (0.461–3.563)	0.63
Above 40	1.00	
Distance from the tumor edge to the articular surface		
<2 mm	4.77 (2.251–10.097)	<0.001
≥2 mm	1.00	
Thickness of the unaffected cortical bone around the tumor		
<3 mm	4.96 (2.337–10.543)	<0.001
≥3 mm	1.00	

5. Conclusion

Our study used a precision-medicine approach to GCTB prognosis, showing that specific CT-derived preoperative information might better aid diagnosis, plan treatment, determine prognosis, and monitor treatment progress. Future prospective studies will test or improve our three-factor model. Its application will enable surgeons to stratify the risk of recurrence preoperatively and early on during outpatient visits. For low-risk patients, psychological distress could be eased, and for high-risk patients, a good model could better characterize the extent of the tumor and potential invasion area, allowing more rigorous preoperative preparation and postoperative review and monitoring.

Funding

This research did not receive any specific grant from funding agencies in the public, commercial, or not-for-profit sectors.

CRediT authorship contribution statement

Lenian Zhou: Conceptualization, Investigation, Formal analysis, Methodology, Data curation, Writing - original draft, Writing - review & editing. **Shanyi Lin:** Investigation, Formal analysis, Methodology, Writing - original draft, Writing - review & editing. **Hanqiang Jin:** Validation, Data curation, Writing - review & editing. **Zhaoyuan Zhang:** Validation, Data curation, Writing - review & editing. **Changqing Zhang:** Conceptualization, Supervision, Methodology, Resources. **Ting Yuan:** Conceptualization, Supervision, Methodology, Resources.

Declaration of Competing Interest

The authors declare that they have no known competing financial interests or personal relationships that could have appeared to influence the work reported in this paper.

Acknowledgements

We sincerely thank Dr. Hongyi Zhu for his assistance in the proofreading of our manuscript, and Ms. Yawen Tang for her assistance in data collection.

Appendix A. Supplementary data

Supplementary data to this article can be found online at https://doi.org/10.1016/j.jbo.2021.100366.

References

[1] N.A. Athanasou, M. Bansal, R. Forsyth, R.P. Reid, Z. Sapi, Giant cell tumour of bone. In: Fletcher CDM, Bridge JA, Hogendoorn PCW, Mertens F, editors., WHO Classification of Tumours of Soft Tissue and Bone Lyon:International Agency for Research on Cancer (2013) 321-324.

[2] A. Al-Ibraheemi, C.Y. Inwards, R.T. Zreik, D.E. Wenger, S.M. Jenkins, J.M. Carter, J.M. Boland, P.S. Rose, L. Jin, A.M. Oliveira, K.J. Fritchie, Histologic Spectrum of Giant Cell Tumor (GCT) of Bone in Patients 18 Years of Age and Below: A Study of 63 Patients, The American journal of surgical pathology 40 (12) (2016) 1702–1712.

[3] C.M. Chan, Z. Adler, J.D. Reith, C.P. Gibbs Jr., Risk factors for pulmonary metastases from giant cell tumor of bone, The Journal of bone and joint surgery, American 97 (5) (2015) 420–428.

[4] Y. He, J. Zhang, X. Ding, Prognosis of local recurrence in giant cell tumour of bone: what can we do?, Radiol. Med. (Torino) 122 (7) (2017) 505–519.

[5] F.M. Klenke, D.E. Wenger, C.Y. Inwards, P.S. Rose, F.H. Sim, Giant cell tumor of bone: risk factors for recurrence, Clin. Orthop. Relat. Res. 469 (2) (2011) 591–599.

[6] C. Errani, P. Ruggieri, M.A. Asenzio, A. Toscano, S. Colangeli, E. Rimondi, G. Rossi, A. Longhi, M. Mercuri, Giant cell tumor of the extremity: A review of 349 cases from a single institution, Cancer Treat. Rev. 36 (1) (2010) 1–7.

[7] R.W. Wysocki, E. Soni, W.W. Virkus, M.T. Scarborough, S.E. Leurgans, S. Gitelis, Is intralesional treatment of giant cell tumor of the distal radius comparable to resection with respect to local control and functional outcome?, Clin. Orthop. Relat. Res. 473 (2) (2015) 706–715.

[8] C.Y. Cheng, H.N. Shih, K.Y. Hsu, R.W. Hsu, Treatment of giant cell tumor of the distal radius, Clinical orthopaedics and related research (383) (2001) 221-8.

[9] W.T. Becker, J. Dohle, L. Bernd, A. Braun, M. Cserhati, A. Enderle, L. Hovy, Z. Matejovsky, M. Szendroi, K. Trieb, P.U. Tunn, Local recurrence of giant cell tumor of bone after intralesional treatment with and without adjuvant therapy, The Journal of bone and joint surgery, American 90 (5) (2008) 1060–1067.

[10] H. Tang, A. Moro, W. Feng, Y. Lai, Z. Xiao, Y. Liu, K. Wang, Giant cell tumors combined with secondary aneurysmal bone cysts are more likely to develop postoperative recurrence: A retrospective study of 256 cases, J. Surg. Oncol. 120 (3) (2019) 359–365.

[11] M. Campanacci, N. Baldini, S. Boriani, A. Sudanese, Giant-cell tumor of bone, The Journal of bone and joint surgery, American 69 (1) (1987) 106–114.

[12] C.M. Costelloe, J.E. Madewell, Radiography in the initial diagnosis of primary bone tumors, AJR Am. J. Roentgenol. 200 (1) (2013) 3–7.

[13] G.H. Prosser, K.G. Baloch, R.M. Tillman, S.R. Carter, R.J. Grimer, Does curettage without adjuvant therapy provide low recurrence rates in giant-cell tumors of bone?, Clinical orthopaedics and related research (435) (2005) 211-8.

[14] S. Purohit, D.N. Pardiwala, Imaging of giant cell tumor of bone, Indian journal of orthopaedics 41 (2) (2007) 91–96.

[15] K.C. Wong, S.M. Kumta, G.E. Antonio, L.F. Tse, Image fusion for computer-assisted bone tumor surgery, Clin. Orthop. Relat. Res. 466 (10) (2008) 2533–2541.

[16] Y. He, J. Wang, J. Zhang, L. Du, Y. Lu, J. Xu, F. Yuan, Y. Tan, X. Ding, Magnetic resonance feature of "paintbrush borders" sign as a novel way to predict recurrence of giant cell tumor of bone after curettage: a pilot study, The Journal of international medical research 46 (2) (2018) 710–722.

[17] T.H. Chen, Y.P. Su, W.M. Chen, Giant cell tumors of the knee: subchondral bone integrity affects the outcome, Int. Orthop. 29 (1) (2005) 30–34.

[18] T. Scholzen, J. Gerdes, The Ki-67 protein: from the known and the unknown, J. Cell. Physiol. 182 (3) (2000) 311–322.

[19] F. Gouin, A.R. Rochwerger, A. Di Marco, P. Rosset, P. Bonnevialle, F. Fiorenza, P. Anract, Adjuvant treatment with zoledronic acid after extensive curettage for giant cell tumours of bone, European journal of cancer (Oxford, England : 1990) 50(14) (2014) 2425-31.

[20] L. Heijden, P.D.S. Dijkstra, M.A.J. Sande, J.R. Kroep, R.A. Nout, C.S.P. Rijswijk, J.V. M.G. Bovée, P.C.W. Hogendoorn, H. Gelderblom, The clinical approach toward giant cell tumor of bone, Oncologist 19 (5) (2014) 550–561.

[21] H. Akaike, Information Theory and an Extension of the Maximum Likelihood Principle, in: E. Parzen, K. Tanabe, G. Kitagawa (Eds.), Selected Papers of Hirotugu Akaike, Springer, New York, New York, NY, 1998, pp. 199–213.

[22] J.E. Fischer, L.M. Bachmann, R. Jaeschke, A readers' guide to the interpretation of diagnostic test properties: clinical example of sepsis, Intensive Care Med. 29 (7) (2003) 1043–1051.

[23] W.G. Ward, Sr., G. Li, 3rd, Customized treatment algorithm for giant cell tumor of bone: report of a series, Clinical orthopaedics and related research (397) (2002) 259-70.

[24] L. van der Heijden, P.D. Dijkstra, D.A. Campanacci, C.L. Gibbons, M.A. van de Sande, Giant cell tumor with pathologic fracture: should we curette or resect?, Clin. Orthop. Relat. Res. 471 (3) (2013) 820–829.

[25] X. Yu, M. Xu, S. Xu, Q. Su, Clinical outcomes of giant cell tumor of bone treated with bone cement filling and internal fixation, and oral bisphosphonates, Oncology letters 5 (2) (2013) 447–451.

[26] J.S. Biermann, W. Chow, D.R. Reed, D. Lucas, D.R. Adkins, M. Agulnik, R.S. Benjamin, B. Brigman, G.T. Budd, W.T. Curry, A. Didwania, N. Fabbri, F.J. Hornicek, J.B. Kuechle, D. Lindskog, J. Mayerson, S.V. McGarry, L. Million, C.D. Morris, S. Movva, R.J. O'Donnell, R.L. Randall, P. Rose, V.M. Santana, R.L. Satcher, H. Schwartz, H.J. Siegel, K. Thornton, V. Villalobos, M.A. Bergman, J.L. Scavone, N.C.C.N. Guidelines, Insights: Bone Cancer, Version 2.2017,, Journal of the National Comprehensive Cancer Network : JNCCN 15 (2) (2017) 155–167.

[27] S. Gitelis, B.A. Mallin, P. Piasecki, F. Turner, Intralesional excision compared with en bloc resection for giant-cell tumors of bone, The Journal of bone and joint surgery, American 75 (11) (1993) 1648–1655.

[28] J. Benevenia, S.M. Rivero, J. Moore, J.A. Ippolito, D.A. Siegerman, K.S. Beebe, F.R. Patterson, Supplemental Bone Grafting in Giant Cell Tumor of the Extremity Reduces Nononcologic Complications, Clin. Orthop. Relat. Res. 475 (3) (2017) 776–783.

[29] F.M. Klenke, D.E. Wenger, C.Y. Inwards, P.S. Rose, F.H. Sim, Recurrent giant cell tumor of long bones: analysis of surgical management, Clin. Orthop. Relat. Res. 469 (4) (2011) 1181–1187.

[30] S. Miwa, T. Otsuka, Practical use of imaging technique for management of bone and soft tissue tumors, Journal of orthopaedic science : official journal of the Japanese Orthopaedic Association 22 (3) (2017) 391–400.

[31] C.S. Wang, J.H. Lou, J.S. Liao, X.Y. Ding, L.J. Du, Y. Lu, L. Yan, K.M. Chen, Recurrence in giant cell tumour of bone: imaging features and risk factors, Radiol. Med. (Torino) 118 (3) (2013) 456–464.

[32] L. Campanacci, A. Sambri, M.R. Medellin, P. Cimatti, C. Errani, D.M. Donati, A new computerized tomography classification to evaluate response to Denosumab in giant cell tumors in the extremities, Acta orthopaedica et traumatologica turcica 53 (5) (2019) 376–380.

[33] Y. He, J. Wang, J. Zhang, F. Yuan, X. Ding, A prospective study on predicting local recurrence of giant cell tumour of bone by evaluating preoperative imaging features of the tumour around the knee joint, Radiol. Med. (Torino) 122 (7) (2017) 546–555.

[34] M.D. Murphey, G.C. Nomikos, D.J. Flemming, F.H. Gannon, H.T. Temple, M.J. Kransdorf, From the archives of AFIP. Imaging of giant cell tumor and giant cell reparative granuloma of bone: radiologic-pathologic correlation, Radiographics : a review publication of the Radiological Society of North America, Inc 21 (5) (2001) 1283–1309.

[35] C.J. Chakarun, D.M. Forrester, C.J. Gottsegen, D.B. Patel, E.A. White, G.R. Matcuk Jr., Giant cell tumor of bone: review, mimics, and new developments in treatment, Radiographics : a review publication of the Radiological Society of North America, Inc 33 (1) (2013) 197–211.

[36] N. Futamura, H. Urakawa, S. Tsukushi, E. Arai, E. Kozawa, N. Ishiguro, Y. Nishida, Giant cell tumor of bone arising in long bones possibly originates from the metaphyseal region, Oncology letters 11 (4) (2016) 2629–2634.

[37] R.L. McGough, J. Rutledge, V.O. Lewis, P.P. Lin, A.W. Yasko, Impact severity of local recurrence in giant cell tumor of bone, Clin. Orthop. Relat. Res. &NA; (438) (2005) 116–122.

[38] Y. Suzuki, Y. Nishida, Y. Yamada, S. Tsukushi, H. Sugiura, H. Nakashima, N. Ishiguro, Re-operation results in osteoarthritic change of knee joints in patients with giant cell tumor of bone, Knee 14 (5) (2007) 369–374.

[39] T. Wang, C.M. Chan, F. Yu, Y. Li, X. Niu, Does Wrist Arthrodesis With Structural Iliac Crest Bone Graft After Wide Resection of Distal Radius Giant Cell Tumor Result in Satisfactory Function and Local Control?, Clin. Orthop. Relat. Res. 475 (3) (2017) 767–775.

[40] C. Zou, T. Lin, B. Wang, Z. Zhao, B. Li, X. Xie, G. Huang, J. Yin, J. Shen, Managements of giant cell tumor within the distal radius: A retrospective study of 58 cases from a single center, Journal of bone oncology 14 (2019) 100211.